Microbial communities in *Caldicellulosiruptor* spp. pretreatment vessels and anaerobic digesters fed dairy manure

Jakob L. Young[1*], Maliea A. Nipko[2], Spencer Butterfield[3], Zachary T. Aanderud[4]

[1]Department of Biology, Brigham Young University, Provo, Utah 84602 USA

[2]Department of Microbiology and Molecular Biology, Brigham Young University, Provo, Utah 84602 USA

[3]Department of Sustainability & Renewable Energy Systems, University of Wisconsin-Platteville, Platteville, Wisconsin, 53818 USA

[4]Department of Plant and Wildlife Sciences, Brigham Young University, Provo, Utah 84602 USA

*Corresponding author: Jakob Young (480) 604-3251 jakyoung@byu.edu

Keywords: Co-occurrence network, community connectivity, biological pretreatment, syntrophic methanogenesis, acetoclastic methanogenesis, methylotrophic methanogenesis

Abstract

The composition of microbial communities was determined in commercial-scale vessels used for 1) hyperthermophilic pretreatment (EBP) of dairy manure with four species of *Caldicellulosiruptor* spp at 70–72ºC, 2) anaerobic digestion of 8% manure in continuously stirred tank reactors (CSTRs) at 35–37°C, and 3) anaerobic digestion at 35-37ºC in induced bed reactors (IBRs) fed a mixture of effluents from EBPs and CSTRs. Samples were collected approximately weekly for 60 days. pH, volatile fatty acid anion and bicarbonate concentrations, COD, and methane yield were measured to assess environmental conditions. Microbial community compositions were obtained via 16S rRNA gene sequencing. *Caldicellulosiruptor* spp. pretreatment altered microbial composition and amplified community connectivity in the IBRs which enhanced syntrophic methanogenesis. Methanobacteriaceae, *Methanobrevibacter*, and *Methanosarcina* were the main methanogenic taxa detected in all reactors. Methanogenic *Methanothermobacter* and Candidatus *Methanoplasma* were uniquely associated with pretreated digestate. Co-occurrence network analysis of pretreated manure in EBP tanks and IBRs revealed dense community interactions, with methylotrophic *Methanosphaera* and hydrogenotrophic *Methanobrevibacter* strongly connected to syntrophic bacteria capable of H_2 production. Raw manure and CSTR community networks were loose and disconnected and exhibited higher modularity. Acetoclastic methanogens did not display co-occurrence relationships with other taxa due to high acetate concentrations in the raw manure and EBP effluent.

Importance

Anaerobic digestion of dairy manure is limited by incomplete hydrolysis of recalcitrant substrates and insufficient syntrophic interaction among microbial taxa. This study examines the impact of hyperthermophilic *Caldicellulosiruptor* spp. pretreatment on microbial community structure and interface across multiple reactor types in a commercial-scale system. Results show that pretreatment

alters methanogenic pathways, selecting for syntrophic archaea and amplifying network connectivity in downstream digesters. These findings provide insights into the microbial basis of improved methane production following pretreatment and suggest network structure as a useful metric for evaluating reactor performance.

Abbreviations

RP	Reception pit
EBP	Extremophilic Biological Process
CSTR	Continuously Stirred Tank Reactor
IBR	Induced Bed Reactor
AD	Anaerobic Digestion or Anaerobic Digestate
VFA	Volatile Fatty Acids
VFAA	Volatile Fatty Acid Anions
TA	Total Alkalinity
COD	Chemical Oxygen Demand
TDS	Total Dissolved Solids
RA	Relative Abundance

1. INTRODUCTION

Anaerobic digestion (AD) relies on microbial metabolism to synthesize biogas consisting almost entirely of CO_2(g) and CH_4(g). Four functional groups of microbes are responsible for the conversion of organic waste into biogas: 1) hydrolytic bacteria, 2) acidogenic bacteria 3) acetogenic and syntrophic bacteria, and 4) methanogenic archaea. However, microbial communities in AD remain poorly understood, especially in the context of large-scale industrial reactors and various pretreatment methods.

Firmicutes and Bacteroidota typically comprise the majority of the microbial community and perform a variety of hydrolytic, acidogenic, and acetogenic roles [1–4]. Members of Actinobacteria and Proteobacteria are involved in the hydrolysis and degradation of complex organic substrates [5,6].

Methanosarcina spp. and *Methanosaeta* spp. are common acetoclastic methanogens that can convert acetate into biogas in a single step catabolic reaction. For example, acetate is converted into methane and bicarbonate [7] by the reaction,

$$CH_3COO^-(aq) + H_2O(l) \rightarrow CH_4(g) + HCO_3^-(aq) \quad (1)$$

Acetoclasts, when acetate concentrations are sufficient for metabolic activity, operate independent of syntrophic relationships with bacteria.

Hydrogenotrophic methanogens, such as members of *Methanobrevibacter*, synthesize methane from H_2 and CO_2 [8,9]. Hydrogenotrophs cannot produce H_2 and require hydrogen gas partial pressures to remain low in solution [10]. To address this limitation, hydrogenotrophic methanogens form relationships with syntrophic bacteria that provide H_2 through direct interspecies hydrogen transfer [11,12]. Hydrogenotrophic methanogenesis occurs via the following coupled reactions [7] that also use acetate as an example,

$$CH_3COO^-(aq) + 4H_2O(l) \rightarrow H_2CO_3(aq) + HCO_3^-(aq) + 4H_2(aq) \quad (2)$$

$$H_2CO_3(aq) + 4H_2(aq) \rightarrow CH_4(g) + 3H_2O(l) \quad (3)$$

Reaction 2 is performed by the syntrophic bacteria, and Reaction 3 is performed by the methanogen. Note that summing Reactions 2 and 3 gives Reaction 1. Hydrogenotrophs can also utilize many other substrates via reactions performed by syntrophic bacteria [13]. For example, butyrate is converted into acetate, CO_2, and H_2 in the reaction,

$$CH_3CH_2CH_2OO^-(aq) + H_2O(l) + HCO_3^-(aq) \rightarrow 2CH_3COO^-(aq) + CO_2(aq) + 2H_2(aq) \qquad (4)$$

The CO_2 and H_2 are then converted into methane by the hydrogenotrophic methanogen via Reaction 3. Note that accumulation of acetate in digesters inhibits Reaction 4. In order to avoid inhibition, substantial activity of acetoclastic methanogens is necessary.

Methylotrophic methanogens, another category of methanogenic archaea, rely on the degradation of methylated compounds, primarily methanol, to produce methane [14]. The chemical reaction responsible for methylotrophic methanogenesis from methanol is as follows [15],

$$4CH_3OH(aq) \rightarrow 3CH_4(g) + CO_2(aq) + 2H_2O\ (l) \qquad (5)$$

Some methanogenic taxa, such as members of *Methanosarcina*, are metabolically flexible and can utilize a combination of acetoclastic, hydrogenotrophic, and methylotrophic methanogenesis depending on metabolite concentrations and environmental conditions [16].

Digester operation is typically monitored by total volatile fatty acid (VFA) concentration, pH, and alkalinity, all of which affect microbial activity and metabolic pathways. A pH range of 6.8-7.5 is optimal for methanogenesis [17,18]. Note that VFAs produced by hydrolysis and acidogenesis all exist as anions at pH 6.8-7.5. Dairy manure is buffered near pH 7.8 by ammonium bicarbonate, so it is critical to monitor bicarbonate concentration. However, alkalinity as measured by titration with HCl includes both bicarbonate and volatile fatty acid anions (VFAAs). Total VFA concentration is commonly reported as acetate equivalents. For an accurate assessment of buffering capacity, the VFAA concentration must be subtracted from the measured alkalinity.

Without pretreatment, biogas yields from AD are limited by incomplete hydrolysis of recalcitrant materials such as lignocellulose and peptidoglycans [19–21]. In this study, the extremophilic biological process (EBP) was employed with *Caldicellulosiruptor* spp. [13,22,23] to increase hydrolysis and acidogenesis, thereby addressing a key limitation in AD of dairy manure. *Caldicellulosiruptor* spp. use exozymes to catalyze hydrolysis of lignin, celluloses, and peptidoglycans and the saccharides released from celluloses are catabolized into acetate. For example,

$$\text{Cellulose} + H_2O(l) \rightarrow C_6H_{12}O_6(aq) \quad (6)$$

$$C_6H_{12}O_6(aq) + 3HCO_3\text{-}(aq) \rightarrow 3CH_3COO\text{-}(aq) + 3H_2CO_3(aq) \quad (7)$$

$$H_2CO_3(aq) \rightarrow H_2O(l) + CO_2(g) \quad (8)$$

Co-occurrence networks are a useful method of visualizing microbial interactions, communities, and detecting possible keystone species [24,25]. Co-occurrence is a measure of the likelihood that two specific taxa are found together in samples more frequently than would be expected by chance. Therefore, a significant co-occurrence value likely represents a meaningful and positive ecological relationship. By testing for co-occurrence between all pairs of detected taxa, a relational network is constructed that illustrates microbial interactions within communities. The metrics, connectivity, eigenvector, and betweenness evaluate the microbial taxa that exert the most influence in a community. Connectivity is a direct measurement of the number of connections a taxon has with other taxa. An eigenvector value is a measure of the connectivity of a particular node in addition to its connections with other highly connected nodes. Nodes with a high eigenvector value are highly central, influential, and likely keystone species in the community [24]. Betweenness is a measure of how often a node lies on the shortest path between all other nodes in a network. Taxa with high betweenness factors often present as bridges in a network and play a large role in the flow of metabolites and substrates in the community. Other metrics represent characteristics of the entire ecological network rather than individual nodes. The

number of components of a network refers to the number of disconnected groups of nodes within the graph. Mean connectivity, the average number of other taxa each taxon is connected to, represents overall network connectivity. Additionally, the clustering coefficient measures the degree to which nodes in the network tend to form tightly clustered groups.

2. MATERIALS AND METHODS

2.1 Site description

The study was conducted at a commercial facility with nine 50,000 gallon anaerobic reactors. Dairy manure was collected in a reception pit (RP) and fed into four extremophilic bacterial process (EBP) tanks at 70–72ºC and two continuously stirred tank reactors (CSTRs) at 35–37ºC. The effluent from all six initial tanks was mixed and fed into three induced bed reactors (IBRs) at 35–37°C. Each reactor had real-time monitoring of temperature, total biogas, and biogas methane content on site. Total methane production was calculated as the product of total biogas and percent methane. The EPBs were inoculated with a mixture of *C. bescii*, *C. owensensis*, *C. acetigenus*, and *C. saccharolyticus*. Hydraulic retention time in all tanks was approximately two days.

2.2 Cultivation of Caldicellulosiruptor spp. *and Inoculum Preparation*

All four *Caldicellulosiruptor* spp. were acquired as lyophilized pellets from the German Collection of Microorganisms and Cell Cultures GmbH (DSMZ). Each culture was revived anaerobically following DSMZ guidelines until the colony reached approximately 2.5×10^6 cells/mL. Specifically, *C. bescii* (DSMZ #6725) was grown in Medium 516 (DSMZ_Medium516.pdf), while *C. owensensis* (DSMZ #13100), *C. saccharolyticus* (DSMZ #8903), and *C. acetigenus* (DSMZ #12137) were each cultivated on Medium 640 (DSMZ_Medium640.pdf). Freezer stocks of each culture were

prepared by mixing 500 µL of cell suspension (≈2.5×10^6 cells/mL) with 500 µL of 60% glycerol in a Don Whitley Scientific miniMACS anaerobic chamber (West Yorkshire, UK). The resulting mixtures were gently agitated at room temperature for 10 minutes, allowing the glycerol to permeate the cells, and then stored at –80°C. For inoculum production, 2 mL each of *C. owensensis*, *C. acetigenus*, *C. saccharolyticus*, and *C. bescii* were added to 1 L of Medium 640 under anaerobic conditions in a miniMACS workstation, followed by incubation at 75°C until the population reached ≈2.5×10^6 cells/mL. Cell density for all cultures was determined by microscopy.

2.3 Sample collection and storage

40 milliliters of sample were gathered from the effluent of each tank approximately weekly over 60 days. Samples were frozen and transported in insulated packaging to the lab at BYU in Provo, Utah for chemical and biological analysis. Samples were kept frozen at -20ºC until analyses. Note that this processing of samples likely increased the measured pH by removing CO_2 from the solution.

2.4 Analyses of samples

A Hannah HI98195 probe (Hannah Instruments, Woonsocket, RI, USA) was used to measure pH. Total VFAs and chemical oxygen demand (COD) were measured with Hach TNT 872 Vial Tests and Hach TNT 822 Vial Tests, respectively (Hach, Loveland, CO, USA). For both VFA and COD measurements, each sample was subsampled, centrifuged for 10 minutes at 4000 RPM, and filtered with an Avantor VWR Syringe Filter (Glass fiber, 13mm, 1.0 um) (Avantor, Radnor Township, PA, USA). Because VFA concentrations in AD effluent tend to be too large for measurement by the Hach TNT Vial Test, each subsample was diluted 10-fold with Milli-Q ultrafiltered water prior to analysis.

Alkalinity was quantified via titration to pH 4 using 1 M HCl on a Hach Instruments TitraLab AT1000 (Loveland, CO, USA). Samples were diluted 100-fold with Milli-Q ultrapure water before titration. Because the measured alkalinity includes both bicarbonate and VFAAs, alkalinity was converted to an estimate of bicarbonate concentration (mg/L) with the equation:

$$\frac{\text{mg } HCO_3^-}{\text{L}} = \left[\frac{\text{Alkalinity}}{\text{50 mg per equivalent}} + \frac{\text{Total VFA}}{\text{59 mg per equivalent}}\right] \times \text{61 mg per equivalent} \quad (9)$$

Alkalinity is expressed as mg $CaCO_3$ equivalents per liter and total VFA is expressed as mg acetate per liter. The constants 50 and 59 represent the mg of $CaCO_3$ and acetate that neutralize one mmole of H^+ ions. The factor 61 is the molar mass of bicarbonate and is used to convert mmol to mg.

2.5 DNA extraction and sequencing

DNA was isolated from 300 mg of each frozen sample using the Qiagen DNEasy PowerWater Kit Pro (Qiagen, Kilden, Germany). Purity and concentration of the extracted DNA were checked with a Nanodrop One Microvolume UV-Vis Spectrophotometer (Thermo Fisher Scientific, Waltham, MA, USA). The 16S rRNA regions coded by the DNA were amplified for sequencing on an Illumina MiSeq platform (Illumina, San Diego, CA, USA), conducted at the Utah State University Sequencing Center in Logan, UT (https://cores.utah.edu/dna-sequencing/).

2.6 DNA sequence processing

All 16S sequences were analyzed using the Qiime2 2022.2 pipeline [26]. First, raw reads were demultiplexed and subjected to quality filtering, removing chimeric reads and applying default denoising parameters. To standardize across samples, data were rarefied to 80,000 reads per sample. Sequences were grouped at 97% similarity and assigned taxonomy via local BLAST against the SILVA

taxonomic database [26,27]. Note that some species will not be detected or identified by the SILVA database [28]. Additionally, DNA presence in a tank does not denote activity [29].

For community dissimilarity, Bray-Curtis distances (Bray & Curtis, 1957) were calculated and visualized with Principal Coordinate Analysis (PCoA). Using the Qiime2R functionality within the tidyverse package, PCoA plots were generated in R (version 4.2.0). Permutational multivariate analysis of variance (PERMANOVA) using the adonis2 function in the vegan package further assessed the statistical significance of between-group differences.

2.6 Microbial correlation testing

Spearman correlations of all taxa abundance and environmental variables (COD, VFA, bicarbonate, pH, total methane production, and tank temperature) were determined. Spearman correlation was used because the microbial abundance data was non-normally distributed, often skewed, and compositional. Due to the rank-based nature of Spearman's correlation, it is less influenced by outliers and suited for detecting nonlinear relationships between microbial taxa and environmental variables. Specifically, for each microbial taxon, abundance of the taxon was tested against COD, VFA, bicarbonate, pH, total methane production, and tank temperature across all samples from all tanks throughout the entire 60-day experiment. This allowed a comprehensive approach to correlation analysis, calculating correlation across the entirety of our data, rather than constraining the correlation to tanks that had changing environmental variables over time. In order to minimize Type I errors given the large number of correlations being tested, the p-values for these tests were adjusted using the Benjamini-Hochberg procedure. This correction reduces the risk of false positives while maintaining statistical power, ensuring that observed correlations reflect meaningful biological trends.

2.7 Microbial co-occurrence networks

The microbial co-occurrence networks were calculated using the cooccur package in R [30]. All detected co-occurrences were filtered for significance ($p < .05$). Taxa unidentified by the SILVA database were removed from the analysis. Networks were calculated using the Fruchterman-Reingold method and a minimum distance was set between nodes to prevent overlap. Distance between nodes was set to the inverse of effect size and the size of nodes was set to node connectivity. The calculated network was plotted using ggraph on R [31]. Connectivity, eigenvector values, and betweenness were calculated for each node. Modularity and connectivity statistics were computed for each graph.

3. RESULTS AND DISCUSSION

3.1 Community compositions

Reception Pit (RP)

The RP tank accepts raw dairy manure that has a stable microbial community (Figure 1, Figure 2). Hydrogenotrophic *Methanobrevibacter* (63.7±2.3%) and Methanobacteriaceae (33.5±2.0%) together dominated the methanogen community (Table 2). *Methanosarcina* (0.3±0.2%), capable of acetoclastic, methylotrophic, and hydrogenotrophic methanogenesis, was relatively low in abundance. Methylotrophic *Methanosphaera* comprised an average relative abundance (RA) of 2.4% of the methanogenic community in the raw manure (Table 2).

Extremophilic Biological Process (EBP)

Firmicutes abundance was constant, comprising the majority of microbes in these tanks (72.9±1.1%), Figure 1. On and around days 10 and 45, the presence of the Thermotogota and Fusobacteriota phyla, which fall under the other category in Figure 1, were noted. *Fusobacteriota* can

specialize in degradation of plant biomass such as cellulose and cellobiose and likely contributed to the hydrolysis of recalcitrant compounds in the EBP tanks [32]. *Thermotogota* are known to prefer higher temperatures and produce H_2, possibly forming relationships with syntrophic methanogens [33,34]. *Methanosarcina* is commonly abundant in manure and digester communities [35], but is unable to grow in hyperthermophilic conditions is therefore below the detection limit in the EBP tanks. As such, *Methanosarcina* displayed a negative correlation with reactor temperature (Spearman's $\rho = -0.38$, $p < .001$, $n = 103$). Note that *Caldicellulosiruptor* spp. are present but not included in the analysis.

As seen in Table 1, the hyperthermophilic EBP reactors have a larger average RA of Euryarchaeota (2.2±0.2% of total) compared with the CSTRs and IBRs. This is explained by two sources of methanogen DNA. Microorganisms from RP have died or gone dormant and their genetic material is detected [36]. Additionally, thermophilic methanogens, e.g. *Methanothermobacter* spp. (6.2±1.5% of methanogens in EBP), from the raw manure grew in the EBP tanks.

Continuously Stirred Tank Reactors (CSTRs)

The CSTRs that were fed manure from the RP, exhibited stable microbial communities of Firmicutes (72.0±0.8%), Bacteroidota (20.8±1.2%), and Actinobacteriota (4.3±0.3%). The main methanogenic taxa were *Methanobrevibacter* (47.8±3.5%), *Methanosarcina* (25.6±4.0%), and Methanobacteriaceae (19.9±1.2%). Of these three methanogenic groups, only Methanobacteriaceae was positively correlated with higher methane yields (Spearman's $\rho = 0.43$, $p = .01$, $n = 54$). Notably, over time, *Methanosarcina* increased in RA in these reactors (Figure 2). *Methanosarcina* spp. are primarily acetoclasts but possess the metabolic flexibility to perform methylotrophic and hydrogenotrophic methanogenesis as well [16,37]. However, despite the high prevalence of *Methanosarcina* in the CSTR tanks, no significant correlation was found between its RA and total methane production.

Methanosarcina is however correlated with lower VFA (Spearman's $\rho = -0.35$, $p < .01$, $n = 103$) and higher bicarbonate (Spearman's $\rho = 0.55$, $p < .001$, $n = 103$) concentrations. In the CSTRs, therefore, *Methanosarcina* sp. actively facilitated acetoclastic methanogenesis, consuming VFAs and releasing bicarbonate, consistent with Reaction 1.

Induced Bed Reactors (IBR)

In the IBR tanks fed a mixture of effluents from the CSTRs and EBP tanks, the RA of Bacteroidota (20.8±1.2%) increased over time, seemingly at the expense of Firmicutes (70.3±0.9%) and Actinobacteriota (4.3±0.3%) (Figure 1, Table 1). The dominant methanogenic taxa in the IBRs were *Methanobrevibacter* (48.7±2.4%), Methanobacteriaceae (26.5±1.7%), and *Methanosarcina* (16.8±2.5%). The RA of *Methanosarcina* in the IBRs was smaller than that of the CSTRs and declined over time (Figure 2). The decreasing RA of *Methanosarcina*, the only acetoclast, denotes a decline in acetoclastic methanogenesis relative to alternative methanogenesis pathways. For example, both methylotrophic methanogens (e.g., Candidatus *Methanoplasma*, 1.0±0.4%), and thermophilic hydrogenotrophic methanogens (e.g., *Methanothermobacter*, 1.6±0.6%), from the raw manure grew in the IBRs. Candidatus *Methanoplasma* was negatively correlated with pH (Spearman's $\rho = -0.28$, $p < .01$, $n = 103$) and positively correlated with methane production (Spearman's $\rho = 0.48$, $p < .001$, $n = 54$). The RA of *Methanothermobacter* unsurprisingly correlated with increased temperatures (Spearman's $\rho = 0.41$, $p < .001$, $n = 103$) and higher methane production (Spearman's $\rho = 0.48$, $p < .001$, $n = 54$). Additionally, hydrogenotrophic *Methanobacterium* (2.4±0.5%) RA steadily declined in the IBRs, disappearing almost entirely by the end of the experiment. *Methanobacterium* was negatively correlated with temperature (Spearman's $\rho = -0.38$, $p < .001$, $n = 103$) and positively correlated with pH (Spearman's $\rho = 0.56$, $p < .001$, $n = 103$), showing a preference for the more alkaline, mesophilic

CSTRs. The evidence from the IBRs indicates EBP pretreatment shifts the methanogenic community away from acetoclastic methanogenesis, likely because IBRs retain large solid particles but allow soluble substrates, such as acetate, to pass through underutilized with low HRT.

3.2 Co-occurrence networks

3.2.1 Reception pit

The RP co-occurrence network was distinct due to its high modularity of 0.74 (Table 3). The community is loosely organized and contains many disconnected groups of taxa (Figure 3). Only members of Firmicutes, Bacteroidota, Actinobacteriota, Euryarchaeota, and Proteobacteria were detected. Methylotrophic *Methanosphaera* and hydrogenotrophic *Methanobrevibacter* are noted in the manure community network but are relatively disconnected and possess low eigenvector values. *Methanosphaera* and *Methanobrevibacter* in raw manure therefore benefit from a few syntrophic relationships to receive H_2 but are not central to the community. The average taxon had a positive relationship with 2.7 other taxa.

3.2.2 EBP tanks

The EBP pretreatment tank co-occurrence network exhibited two highly dense and interconnected communities (Figure 3). Each taxon in the EBP tanks was connected to an average of 16.6 other taxa (Table 3). The network had a modularity value of 0.5. Members of Firmicutes and Bacteroidota, including *Herbinix* and *Petrimonas* genera, comprised the majority of taxa with high eigenvector values. Notably, the third most influential taxon in the EBP tanks was a member of the Verrucomicrobiota phylum, presenting with an eigenvector of 0.995. Methylotrophic *Methanosphaera* and hydrogenotrophic *Methanobrevibacter* displayed centrality in the community, both exhibiting

relatively high eigenvector and degree values. Both *Methanosphaera* and *Methanobrevibacter* exhibited strong co-occurrence relationships with syntrophic bacteria capable of H_2 production, notably members of Thermoanaerobacteraceae, Thermovenabulum, and *Caldicoprobacter* [38–40]. Dong et al. (2018) established that hyperthermophilic temperatures in AD cause a shift towards hydrogenotrophic methanogens and the formation of strong syntrophic relationships with bacteria [41]. *Methanosarcina*, the only acetoclastic genus detected in the system, was detected in very low abundance (Table 2) and did not display positive co-occurrence with any identified bacterial taxa. However, acetoclastic methanogens capable of withstanding the high temperatures would be expected to form a close syntrophic relation with the *Caldicellulosiruptor* spp. in the EBP tanks due to their acetate production (Reactions 6 and 7).

3.2.3 CSTRs

The CSTR network had a modularity value of 0.57 and consisted of 3 components (Table 3). The most influential taxa with the highest eigenvector values were entirely of the *Firmicutes* phylum. Despite being detected in large RA (Table 1), no positive relationships toward methanogenic taxa were detected in the CSTR tanks. Many known acetogenic taxa, such as Lachnospiraceae and *Syntrophomonas*, presented with high betweenness factors [42,43]. Acetogenic taxa therefore played a key role in this community, transforming the products of related hydrolytic and acidogenic bacteria into acetate for methanogenesis. The high rate of production of acetate by these organisms likely contributed to the lack of acetoclastic *Methanosarcina* in the network, as acetate was readily available in the digestate. The lack of hydrogenotrophic methanogens in the network, however, suggests a fundamental limitation to their methane production due to their reliance on interspecies hydrogen transfer [12].

3.2.4 IBRs

In the IBRs fed a mixture of about one-third CSTR effluent and two-thirds EBP effluent, the IBR co-occurrence network had a modularity value of 0.43 and each taxon in the network was connected to 11.69 taxa on average (Table 3). Methylotrophic *Methanosphaera* exhibited both the highest betweenness factor in this community and a high eigenvector value (0.8) indicating *Methanosphaera* was a keystone species in this community, forming a tight syntrophic web with a diverse consortium of bacteria. In particular, due to its hydrogen-dependence, *Methanosphaera* formed strong relationships with syntrophic bacteria known to produce H_2, such as members of Thermoanaerobacteraceae, *Defluviitoga*, and *Caldicoprobacter* [38,39,44]. No acetoclastic methanogens presented in the co-occurrence network, indicating catabolism of acetate produced in the EBP tanks. However, despite elevated VFAA concentrations in the IBRs, no difference was discerned between the bicarbonate concentrations of the CSTRs and IBRs (Tukey, $\Delta = -198.53$, $p > 0.05$). Acetoclastic activity, therefore, was not sufficient to convert the elevated acetate concentrations into additional methane and bicarbonate, as seen in Reaction 1.

3.2.5 Comparison of networks

The RP network was the most disconnected, exhibiting the highest modularity (0.74) and lowest mean connectivity value (2.7). Although the CSTR community had slightly higher connectivity (3.93) than RP, its overall structure resembled that of the RP. In contrast, the EBP and IBR communities exhibited much higher connectivity and resembled each other. The EBP tanks have the highest connectivity value (16.6) of all tanks and the IBR network has a connectivity value of 11.69. Both the EBP and IBR networks consisted of 1 component, while the RP and CSTR consisted of multiple components. The EBP and IBR networks have clustering coefficients of 0.6, larger than both the RP

(0.44) and CSTRs (0.38). While the most influential members of the CSTR network were entirely Firmicutes, the most influential taxa in both the EBP and IBR networks were more diverse, consisting of Firmicutes, Bacteroidota, and others. Additionally, a member of the Verrucomicrobiota phylum was highly influential in both EBP and IBR networks. Notably, the IBR network had the lowest modularity value (0.43), indicating that its community was the least segmented into disconnected subgroups among all tank types. Except the CSTRs, syntrophic methanogens exhibited relationships with other taxa in all other networks. Acetoclastic *Methanosarcina* did not have co-occurrence relationships in any of the tanks due to the high levels of acetate from the RP and EBP effluent.

3.3 Community dissimilarity and relationship with environmental variables

Dissimilarities between microbial community compositions, i.e. all of the detected taxa in a sample weighted according to their RA, were assessed between tank types using PCoA (Figure 4). The strength and direction of the correlations among significant environmental variables and community compositions is overlaid as vectors. Microbial communities differed by tank type (PERMANOVA, $R^2 = 0.36$, $p < .001$). Axis 1, with 40.42% variance explained, largely differentiated communities by VFA and bicarbonate concentrations. Additionally, axis 1 horizontally separated the reactors responsible for methane production (CSTRs and IBRs) from the raw manure and pretreatment tanks (RP and EBP tanks). Axis 2, with 13.29% variance explained, vertically differentiated communities by pH, COD, temperature, and TDS.

The dissimilarities between the communities identified across tank types provide insights on the shifts in microbial communities and metabolic activities over time. Near the beginning of the experiment, communities in the EBP tanks were associated with higher COD, temperature, and pH. But these communities progressively became more associated with high VFA and low bicarbonate

concentrations as time passed, in line with *Caldicellulosiruptor* activity (Reactions 6, 7, and 8). During the experiment, the EBP communities evolved to become similar to the raw manure communities in the RP (Figure 4). Conversely, CSTR and IBR communities were notably different from those of the RP and EBP and were distinctly correlated with higher bicarbonate concentrations, indicating active methanogenic communities, i.e., see Reactions 1, 2, and 3. At the start of the experiment, the CSTRs and IBRs were similar (Figure 4), but the IBR communities became distinct due to the introduction of EBP effluent which contains significant amounts of acetate (Figure 5). The EBP effluent was dominated by thermophiles not suitable for activity in the mesophilic IBRs. Consequently, the microbial community that developed in the IBRs over time was shaped by both the physiochemical characteristics of the EBP effluent and the community in the CSTR effluent, ultimately resulting in a community distinct from both the EBP and CSTR communities. Also, as the experiment progressed, the IBR communities became more correlated with increased TDS and decreased pH. The association with decreased pH was due to syntrophic activity replacing bicarbonate with acetate as seen in Reaction 4. Additionally, despite being rich in acetate, EBP effluent did not contain active acetoclastic methanogens responsible for the conversion of acetate into bicarbonate (Reaction 1) which would stabilize pH. The design of IBRs retains large particles which accounts for the correlation with increased TDS.

3.4 Correlations of bacterial phyla and methanogenic genera with environmental variables

Environmental variables varied substantially between tank types (Figure 5). EBP-pretreated digestate had lower pH and higher VFAA concentrations than raw manure in the RP (Tukey, $\Delta = 0.202$, $p = 0.019$), see Figure 5. VFAA concentrations varied between tanks (ANOVA, $F(3,25) = 36.382$, $p < 0.001$), with higher VFAA levels in EBP tanks compared to the CSTRs (Tukey, $\Delta = 4797.614$, $p < 0.001$) and IBRs (Tukey, $\Delta = 1793.985$, $p < 0.05$) due to *Caldicellulosiruptor* spp. activity (Reactions 6

and 7). Bicarbonate varied across tank types (ANOVA: $F(3,25) = 10.10$, $p < 0.001$), with EBP exhibiting lower bicarbonate concentrations and thence less buffering capacity than both the CSTRs (Tukey, $\Delta = -3584.87$, $p < 0.001$) and the IBRs (Tukey, $\Delta = -3386.34$, $p < 0.001$). *Caldicellulosiruptor* spp. actively convert bicarbonate into carbon dioxide, as seen in Reactions 7 and 8, explaining the low levels of bicarbonate detected in these tanks. Bicarbonate concentrations were highest in the CSTR and IBR tanks, because bicarbonate is a product of both acetoclastic (Reaction 1) and hydrogenotrophic (Reactions 2 and 3) methanogenic activity. pH levels differed across tank types over time (ANOVA: $F(3,25) = 4.353$, $p < 0.001$), with EBP pretreatment tanks exhibiting the most acidic environment due to the high VFAA and low bicarbonate concentration. The pH in the IBRs declined over time because syntrophic bacteria removed bicarbonate and released acetate, as shown in Reaction 4.

Correlation analysis shows that members of the Firmicutes phylum prefer more alkaline pH (>8.25) and are inhibitory to methanogenesis. For example, Clostridiaceae *Clostridium* (Spearman's $\rho = 0.28$, $p < .01$, $n = 103$), Hungateiclostridiaceae *Fastidiosipila* (Spearman's $\rho = 0.25$, $p < .05$, $n = 103$), and Hungateiclostridiaceae *HN-HF0106* (Spearman's $\rho = 0.34$, $p < .01$, $n = 103$) display a preference for higher pH environments. *Romboutsia* (Spearman's $\rho = -0.52$, $p < 0.001$, $n = 54$), *Turicibacter* (Spearman's $\rho = -0.53$, $p < 0.001$, $n = 54$), *Atopostipes* (Spearman's $\rho = -0.65$, $p < 0.001$, $n = 54$), *Clostridium* (Spearman's $\rho = -0.48$, $p < 0.001$, $n = 54$), and *Corynebacterium* (Spearman's $\rho = -0.51$, $p < 0.01$, $n = 54$) show a negative correlation with total methane production, suggesting proliferation of these taxa are inhibiting methanogenesis. Greater abundance of Bacteroidota compared to *Firmicutes* has been shown to increase digester stability and methane yield [1]. A similar trend was identified in our data, with the highest biogas yield coming from IBR tanks with Bacteroidota RA > 20% (Table 1).

In general, members of the Actinobacteria phylum preferred lower pH, lower bicarbonate concentrations, and higher temperatures. Actinobacteria are strongly correlated with the lower pH

environments in the EBP and IBR tanks, *Micrococcales* spp. (Spearman's $\rho = -0.39$, $p < .001$, $n = 103$); members of *Nocardioidaceae* (Spearman's $\rho = -0.39$, $p < .05$), and *Bifidobacteriaceae Bifidobacterium* (Spearman's $\rho = -0.37$, $p < .05$, $n = 103$).

Methanobacterium and *Methanosarcina* both correlated with low VFAA concentration, high bicarbonate, and low temperature. The negative correlation to pH suggests that these methanogenic taxa prefer the IBRs as opposed to the CSTRs. All other members of the *Euryarchaetoa* phylum correlated with the opposite, high VFAA concentration, low bicarbonate, high temperature, and higher total methane production. *Methanobacterium* uniquely displays a negative correlation with total methane production. The RA of Methanobacteriaceae (Spearman's $\rho = -0.50$, $p < .001$, $n = 103$), more specifically *Methanosphaera* (Spearman's $\rho = -0.31$, $p < .01$, $n = 103$), had a strong correlation with decreasing pH in the ADs. The abundance of *Methanothermobacter* (Spearman's $\rho = -0.42$, $p < .01$, $n = 103$) was also correlated with decreasing pH, although this may reflect the taxon's preference for the thermophilic conditions in the EBP tanks rather than lower pH.

4. CONCLUSIONS

EBP pretreatment causes acetate accumulation and elevated methane production in downstream reactors. The RA of *Methanosarcina*, the only acetoclastic genus detected in the studied system, grew substantially in the CSTRs processing raw manure. Although the IBRs continuously received a mixture of *Methanosarcina*-rich CSTR effluent and acetate-rich EBP effluent, the RA of *Methanosarcina* in the IBRs declined. Also, note that *Methanosarcina* were absent from the IBR co-occurrence networks showing they did not rely on syntrophic relationships. Instead, *Methanosarcina* apparently relied on acetate produced by the EBP and a variety of bacterial sources. Because of the declining RA of

acetoclasts and very short HRT in the IBRs, the high acetate levels in the pretreated digestate are underutilized and the higher methane production in the IBRs is due to the growth in RA of hydrogenotrophic methanogens, as opposed to acetoclasts.

The co-occurrence networks in the EBP and IBR tanks had considerably higher mean connectivity and clustering values than untreated manure in the RP and CSTRs. Both EBP and IBR networks consisted of one tightly interconnected component, while RP and CSTR networks were disconnected and contained many components of different taxa. Within the EBP and IBR networks, hydrogenotrophic *Methanobrevibacter* and methylotrophic *Methanosphaera* genera were central in these communities with high connectivity and eigenvector values. Both *Methanobrevibacter* and *Methanosphaera* formed strong connections with known H_2-producing bacteria, such as members of *Caldicoprobacter*. In contrast, no positive co-occurrence relationships with hydrogenotrophic methanogens were detected in the CSTRs. Additionally, while present in the EBP tanks, the RA of methylotrophic Candidatus *Methanoplasma* grew in the IBRs.Therefore, EBP causes physiochemical changes in substrate that ultimately selects for hydrogenotrophic and methylotrophic methanogens and the syntrophic bacteria with which they actively cooperate.

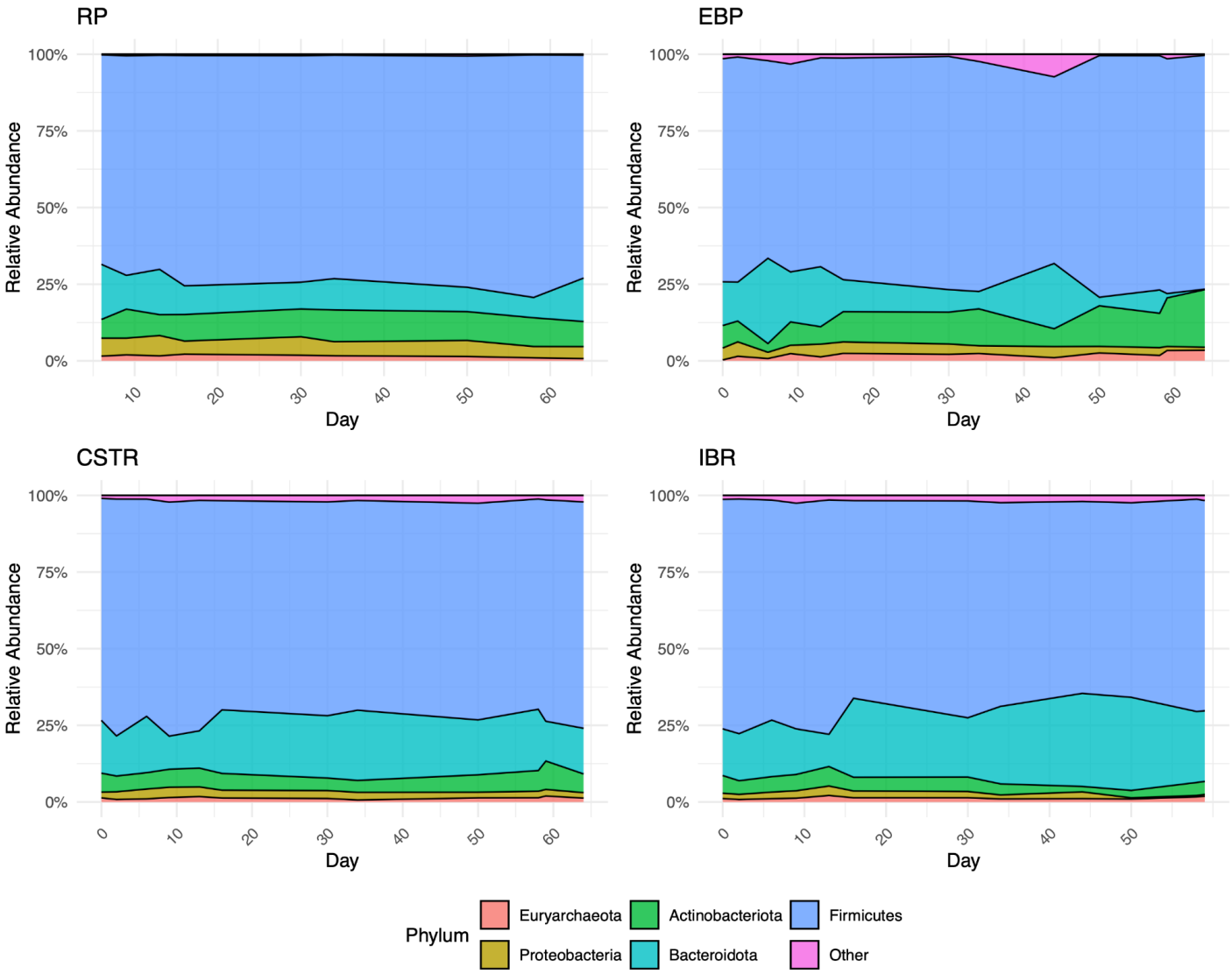

Figure 1. Stacked area plots showing relative abundance of the five most common microbial phyla in each tank type over time. The abundance values represent the average across all tanks within each category by date. See Table 1. Bacteroidota relative abundance decreases in the EBP tanks and increases in the IBRs. Actinobacteria relative abundance increases in the EBP tanks.

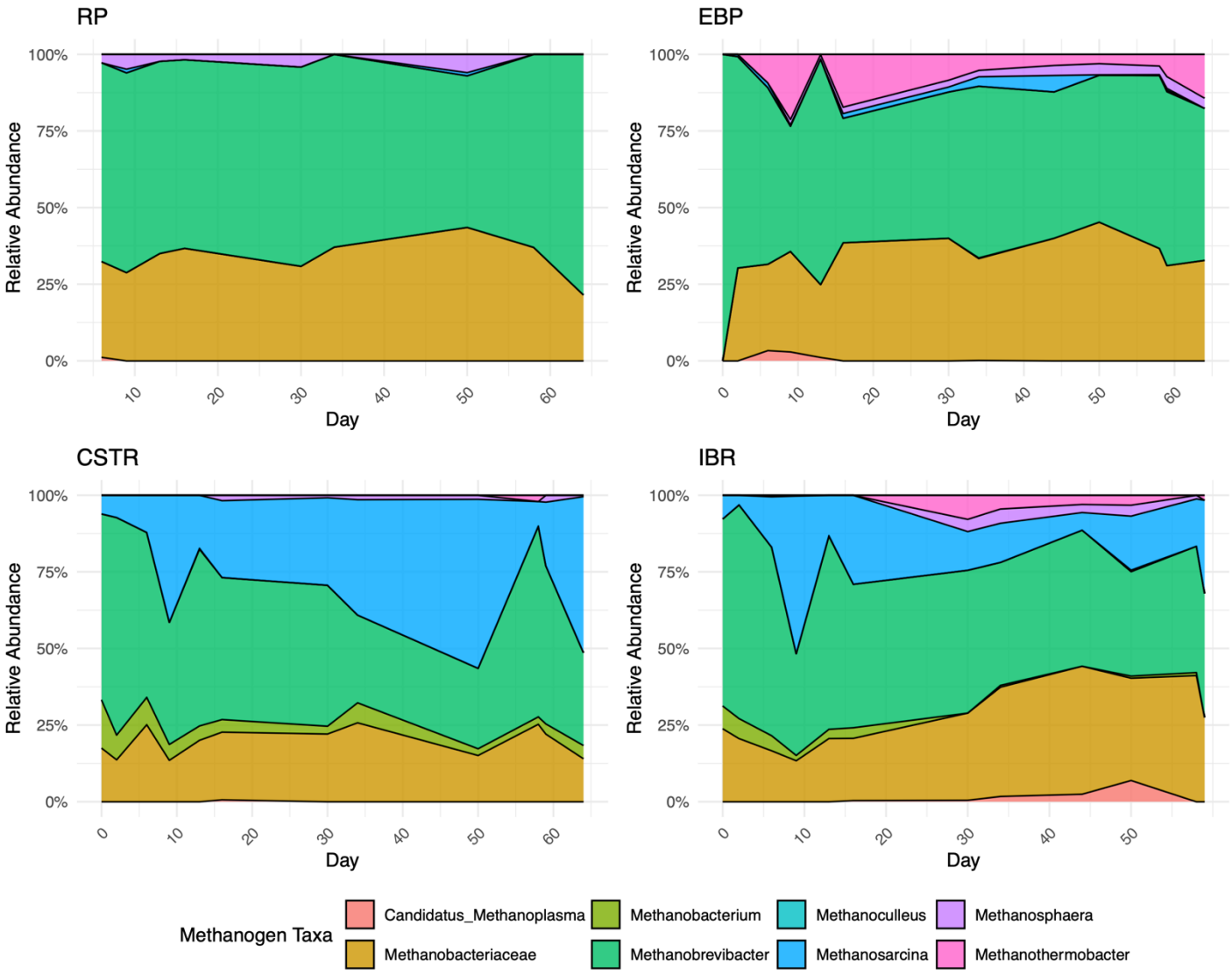

Figure 2. Stacked area plot depicting the community abundance of methanogenic archaea over time across the three tank categories and the Reception Pit (RP). Abundances are averages across all tanks within the category on that date. See Table 2. Hydrogenotrophic methanogens dominate all communities. Acetoclastic *Methanosarcina* sp. relative abundance grows in the CSTRs and declines in the IBRs. Methylotrophic and thermophilic methanogen relative abundance grows in the IBRs.

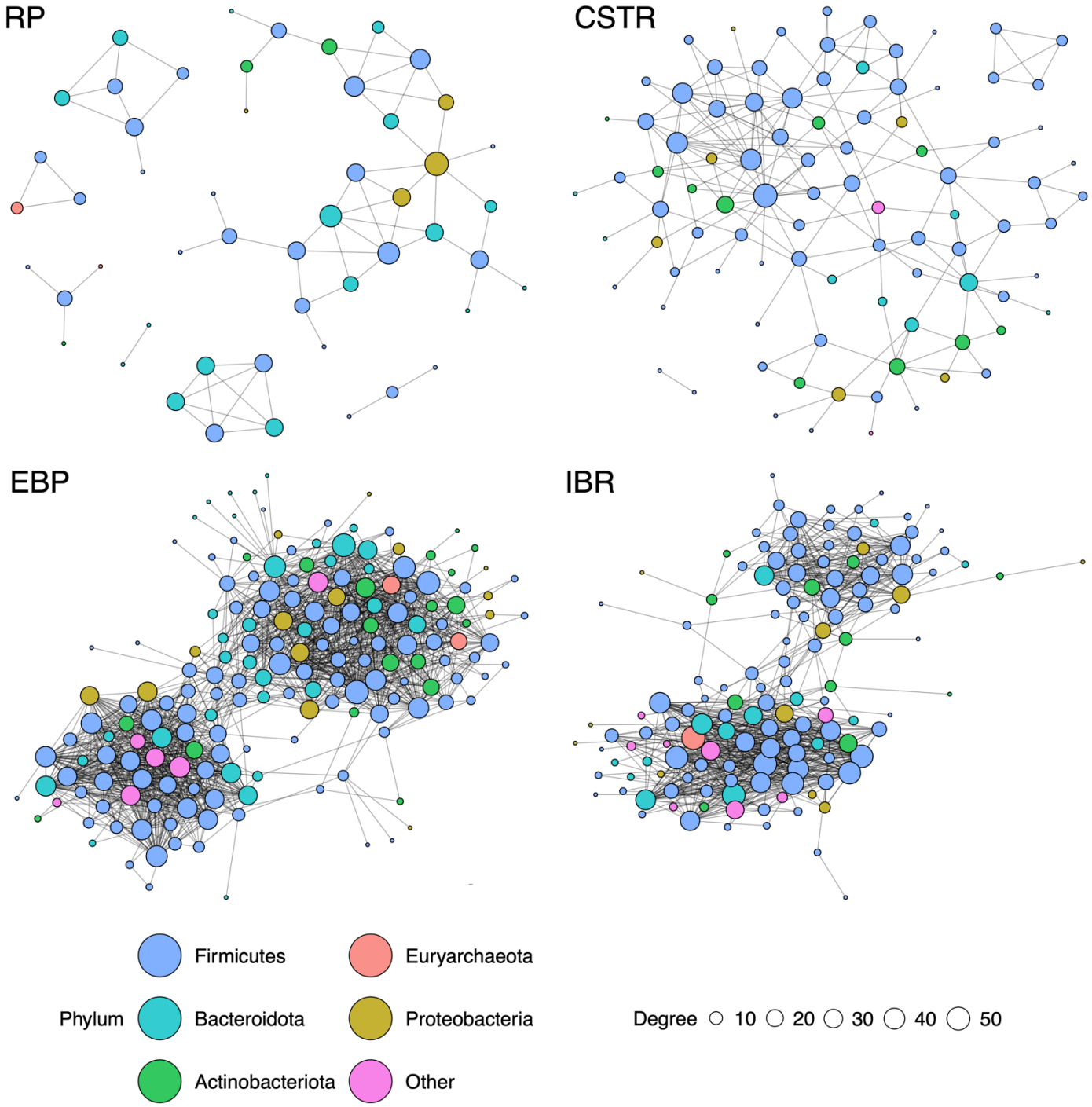

Figure 3. Co-occurrence network graphs depicting community relationships between microbial taxa in the RP (n = 10), EBP tanks (n = 37), IBRs (n = 33), and CSTRs (n = 23). Lines are drawn between taxa when they are observed together in samples significantly more frequently than random ($p < .01$). The

closeness between a pair of taxa corresponds with the effect size of the relationship. The size of the node represents the number of connections to other taxa. See Table 3 for network statistics. EBP and IBR networks are dense and interconnected, with hydrogenotrophic methanogens central to their communities. Raw manure (RP) and CSTR communities are disconnected and indistinct. No co-occurrence relationships with methanogenic taxa were detected in the CSTR tanks.

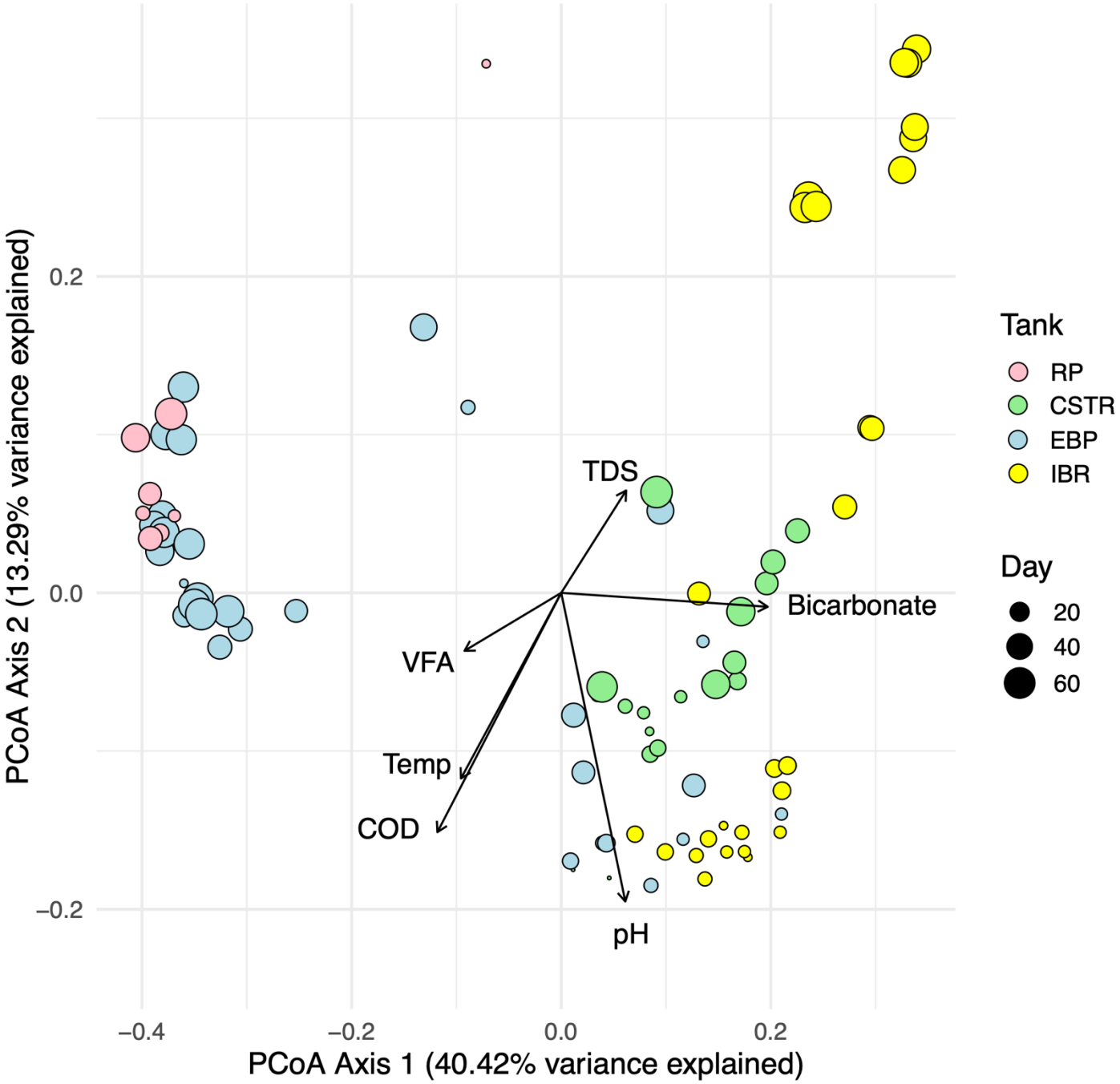

Figure 4. Principal Coordinates Analysis (PCoA) biplot of microbial community composition in all samples with colors corresponding to tank type. Point sizes indicate when the sample was collected with smaller points represent samples collected near the beginning of the experiment while the larger points

represent samples collected near the end of the experiment. A point represents the microbial community composition of a sample, i.e. all of the detected taxa in a sample weighted according to their relative abundance. Vectors depict significant correlations with environmental variables and microbial community compositions. The length of each vector indicates the strength of the correlation with each of the environmental variables, total dissolved solids (TDS), volatile fatty acids (VFA), temperature (Temp), pH, and bicarbonate. Reactors responsible for methane production (CSTRs and IBRs) and tanks responsible for pretreatment and storing manure (EBP tanks and RP) are separated by Axis 1. Both the EBP and IBR communities experienced change over time, are correlated with decreasing pH. EBP tanks and IBRs were similar in the beginning but diverged with time. EBP tanks followed the diagonal from the lower right to upper left. IBRs followed a vertical path, aligned with axis 2, moving from the bottom right to the top right. RP and CSTR community compositions did not substantially change over time.

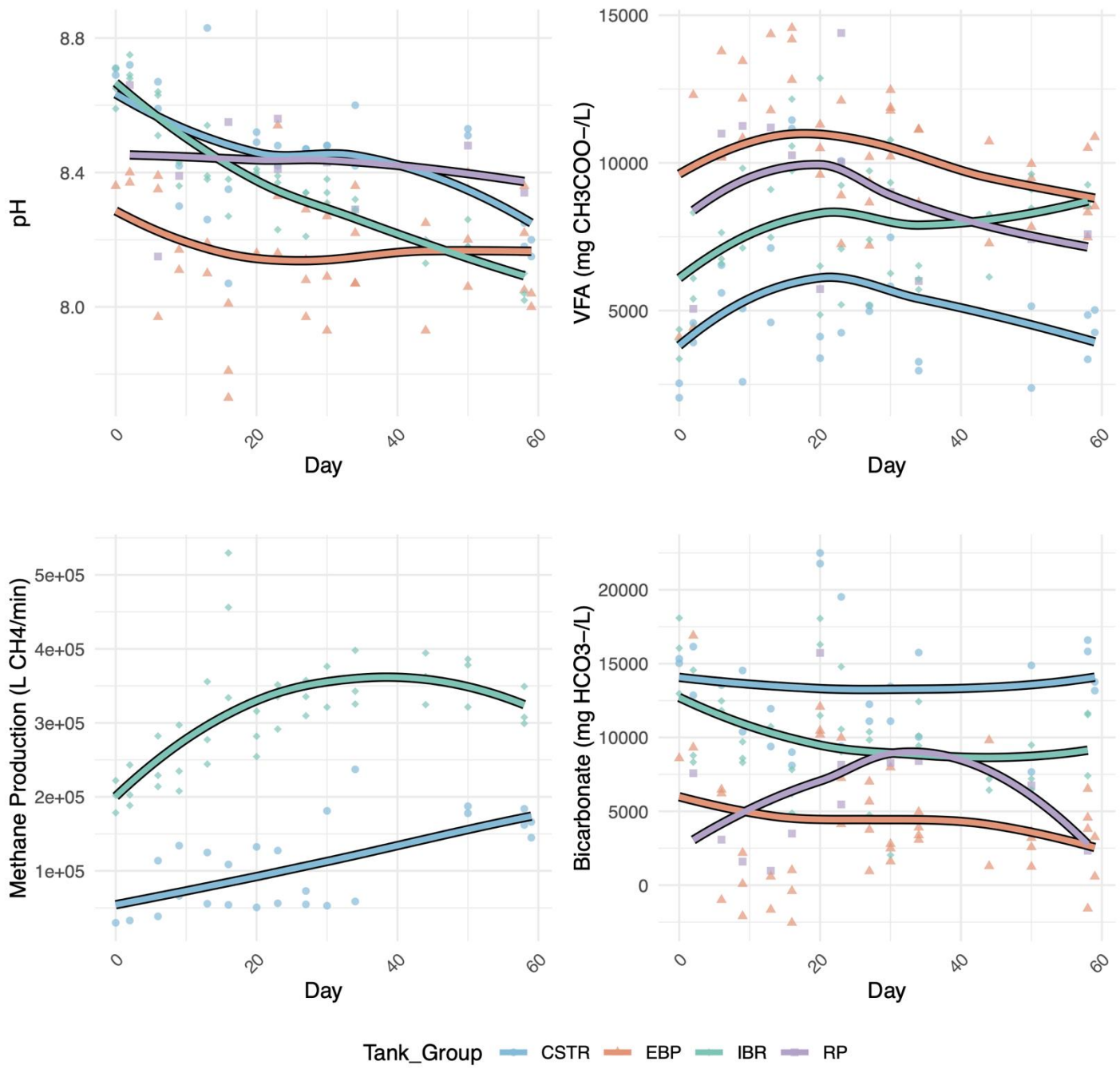

Figure 5. Trends in pH, Total VFA, bicarbonate, and methane gas flow (L/min) by tank type over time. Regressions are calculated and drawn using the Locally Estimated Scatterplot Smoothing (LOESS) technique to clearly illustrate trends in variables over time. EBP tanks consistently had lower pH and

bicarbonate, and higher total VFAA concentrations than other tanks. IBRs exhibited decreasing pH and increasing VFAA concentrations over time. CSTRs had higher bicarbonate concentrations and lower total VFA concentrations than other tanks. IBRs consistently produced more methane on average than the CSTRs.

Table 1. Summary of non-methanogenic community composition by mean relative abundance of phyla across samples, separated by RP (n = 10), EBP tanks IBRs (n = 33), and CSTRs (n = 23). Since the relative abundance is averaged from all samples throughout the experiment, standard error is included. See Figure 1.

Phylum	**RP** 1 tank, n = 10	**EBP** 4 tanks, n = 37	**CSTR** 2 tanks, n = 23	**IBR** 3 tanks, n = 33
Firmicutes	66.8% ± 6.5	72.9% ± 1.1	72.0% ± 0.8	70.3% ± 0.9
Bacteroidota	11.6% ± 1.2	10.4% ± 1.6	16.9% ± 1.0	20.8% ± 1.2
Actinobacteriota	9.7% ± 1.2	10.5% ± 0.9	5.8% ± 0.3	4.3% ± 0.3
Proteobacteria	9.6% ± 4.6	2.6% ± 0.2	2.5% ± 0.1	1.8% ± 0.2
Euryarchaeota	1.4% ± 0.2	2.2% ± 0.2	1.3% ± 0.1	1.3% ± 0.1
Other	0.8% ± 0.4	1.5% ± 0.4	1.5% ± 0.1	1.5% ± 0.1

Table 2. Summary of methanogen community composition by mean relative abundance across samples, separated by tank type. The relative abundance is presented as the percentage of the methanogenic community. Since the relative abundance is averaged from all samples throughout the experiment, standard error is included. See Figure 2.

Methanogen	**Methanogenic Pathway**	**RP** 1 tank, n = 10	**EBP** 4 tanks, n = 37	**CSTR** 2 tanks, n = 23	**IBR** 3 tanks, n = 33
Methanobrevibacter sp.	Hydrogenotrophic[b]	63.7% ± 2.3	56.3% ± 2.7	47.8% ± 3.5	48.7% ± 2.35
Methanobacteriaceae	Mostly Hydrogenotrophic	33.5% ± 2.0	33.5% ± 1.7	19.9% ± 1.2	26.5% ± 1.74
Methanosarcina sp.	Acetoclastic and Hydrogenotrophic[c]	0.3% ± 0.2	1.2% ± 0.4	25.6% ± 4.0	16.8% ± 2.49
Methanothermobacter sp.	Hydrogenotrophic[d]	**ND**[a]	6.2% ± 1.5	0.1% ± 0.1	1.6% ± 0.57
Methanobacterium sp.	Hydrogenotrophic[e]	**ND**	**ND**	5.5% ± 0.9	2.4% ± 0.5
Methanosphaera sp.	Methylotrophic[f]	2.4% ± 0.7	2.0% ± 0.3	0.5% ± 0.2	1.4% ± 0.4
Candidatus *Methanoplasma*	Methylotrophic[g]	0.1% ± 0.1	0.4% ± 0.2	**ND**	1.0% ± 0.4

a. **ND = Not Detected**
b. [45]
c. [16]
d. [41]
e. [46]
f. [47]
g. [48]

Table 3. Co-occurrence network summary statistics by tank type. Components refer to the number of disconnected groups of taxa in a community. Modularity measures how well a network divides into communities with dense internal and sparse external connections. Mean Connectivity is the average number of taxa each taxon is connected to within a network. Mean clustering represents the degree to which nodes in a network tend to cluster together into tight groups.

Parameter	**RP**	**EBP**	**CSTR**	**IBR**
Components	7	1	3	1
Modularity	0.74	0.51	0.57	0.44

Mean Connectivity	2.70 ± 0.21	16.58 ± 1.00	3.93 ± 0.32	11.70 ± 0.94
Mean Clustering	0.44 ± 0.05	0.60 ± .02	0.38 ± .04	0.60 ± .03

ACKNOWLEDGMENTS

The authors thank Lee D. Hansen and Jaron C. Hansen for their assistance with both editing and experimental design. We also acknowledge the help of Jane Allen, Celeste Doxey, Katie Tano, Meredith Murdock, Zachary Fears, Kailey Condie, and Lauren Membreño with sample processing.

Literature Cited

1. Chen S, Cheng H, Wyckoff KN *et al.* Linkages of *Firmicutes* and *Bacteroidetes* populations to methanogenic process performance. *J Ind Microbiol Biotechnol* 2016;**43**:771–81.

2. Giongo A, Granada CE, Borges LGA *et al.* Microbial communities in anaerobic digesters change over time and sampling depth. *Braz J Microbiol* 2020;**51**:1177–90.

3. Kirkegaard RH, McIlroy SJ, Kristensen JM *et al.* The impact of immigration on microbial community composition in full-scale anaerobic digesters. *Sci Rep* 2017;**7**:9343.

4. Shah FA, Mackie RI, Mahmood Q. Biogas Dynamics and Microbial Composition Employing Different Inocula and Substrates in Continuous Stirred-Tank Reactors. *Microbiol Res* 2024;**15**:174–86.

5. Lacombe-Harvey M-È, Brzezinski R, Beaulieu C. Chitinolytic functions in actinobacteria: ecology, enzymes, and evolution. *Appl Microbiol Biotechnol* 2018;**102**:7219–30.

6. Nzeteu C, Joyce A, Thorn C *et al.* Resource recovery from the anaerobic digestion of food waste is underpinned by cross-kingdom microbial activities. *Bioresour Technol Rep* 2021;**16**:100847.

7. Kurade MB, Saha S, Salama E-S *et al.* Acetoclastic methanogenesis led by *Methanosarcina* in anaerobic co-digestion of fats, oil and grease for enhanced production of methane. *Bioresour Technol* 2019;**272**:351–9.

8. Tanikkul P, Phalakornkule C, Champreda V *et al.* Comparative Granular Characteristics of Mesophilic and Thermophilic UASB Producing Biogas from Palm Oil Mill Effluent. *Chem Eng Trans* 2016;**50**:205–10.

9. Zhu X, Treu L, Kougias PG *et al.* Converting mesophilic upflow sludge blanket (UASB) reactors to thermophilic by applying axenic methanogenic culture bioaugmentation. *Chem Eng J* 2018;**332**:508–16.

10. Demirel B, Scherer P. The roles of acetotrophic and hydrogenotrophic methanogens during anaerobic conversion of biomass to methane: a review. *Rev Environ Sci Biotechnol* 2008;**7**:173–90.

11. Stams AJM, Plugge CM. Electron transfer in syntrophic communities of anaerobic bacteria and archaea. *Nat Rev Microbiol* 2009;**7**:568–77.

12. Junicke H, Feldman H, Van Loosdrecht MCM *et al.* Limitation of syntrophic coculture growth by the acetogen. *Biotechnol Bioeng* 2016;**113**:560–7.

13. Hansen LD. Thermodynamic method for analyzing and optimizing pretreatment/anaerobic digestion systems. *Biofuel Res J* 2023;**10**:1816–29.

14. Bueno de Mesquita CP, Wu D, Tringe SG. Methyl-Based Methanogenesis: an Ecological and Genomic Review. *Microbiol Mol Biol Rev* 2023;**87**:e00024-22.

15. Glass JB, Whitman WB. Methanogenesis. In: Gargaud M, Irvine WM, Amils R, et al. (eds.). *Encyclopedia of Astrobiology*. Berlin, Heidelberg: Springer, 2019, 1–6.

16. De Vrieze J, Hennebel T, Boon N *et al.* Methanosarcina: the rediscovered methanogen for heavy duty biomethanation. *Bioresour Technol* 2012;**112**:1–9.

17. Atasoy M, Cetecioglu Z. The effects of pH on the production of volatile fatty acids and microbial dynamics in long-term reactor operation. *J Environ Manage* 2022;**319**:115700.

18. Franke-Whittle IH, Walter A, Ebner C *et al.* Investigation into the effect of high concentrations of volatile fatty acids in anaerobic digestion on methanogenic communities. *Waste Manag* 2014;**34**:2080–9.

19. Atelge MR, Atabani AE, Banu JR *et al.* A critical review of pretreatment technologies to enhance anaerobic digestion and energy recovery. *Fuel* 2020;**270**:117494.

20. Bandgar PS, Jain S, Panwar NL. A comprehensive review on optimization of anaerobic digestion technologies for lignocellulosic biomass available in India. *Biomass Bioenergy* 2022;**161**:106479.

21. Khanh Nguyen V, Kumar Chaudhary D, Hari Dahal R *et al.* Review on pretreatment techniques to improve anaerobic digestion of sewage sludge. *Fuel* 2021;**285**:119105.

22. Hansen JC, Aanderud ZT, Reid LE *et al.* Enhancing waste degradation and biogas production by pre-digestion with a hyperthermophilic anaerobic bacterium. *Biofuel Res J* 2021;**8**:1433–43.

23. Straub CT, Khatibi PA, Otten JK *et al.* Lignocellulose solubilization and conversion by extremely thermophilic Caldicellulosiruptor bescii improves by maintaining metabolic activity. *Biotechnol Bioeng* 2019;**116**:1901–8.

24. Berry D, Widder S. Deciphering microbial interactions and detecting keystone species with co-occurrence networks. *Front Microbiol* 2014;**5**, DOI: 10.3389/fmicb.2014.00219.

25. Rawstern AH, Hernandez DJ, Afkhami ME. Central Taxa Are Keystone Microbes During Early Succession. *Ecol Lett* 2025;**28**:e70031.

26. Bolyen E, Rideout JR, Dillon MR *et al.* Reproducible, interactive, scalable and extensible microbiome data science using QIIME 2. *Nat Biotechnol* 2019;**37**:852–7.

27. Quast C, Pruesse E, Yilmaz P *et al.* The SILVA ribosomal RNA gene database project: improved data processing and web-based tools. *Nucleic Acids Res* 2013;**41**:D590-596.

28. Hugerth LW, Andersson AF. Analysing Microbial Community Composition through Amplicon Sequencing: From Sampling to Hypothesis Testing. *Front Microbiol* 2017;**8**, DOI: 10.3389/fmicb.2017.01561.

29. Blazewicz SJ, Barnard RL, Daly RA *et al.* Evaluating rRNA as an indicator of microbial activity in environmental communities: limitations and uses. *ISME J* 2013;**7**:2061–8.

30. Griffith DM, Veech JA, Marsh CJ. **cooccur** : Probabilistic Species Co-Occurrence Analysis in *R. J Stat Softw* 2016;**69**, DOI: 10.18637/jss.v069.c02.

31. Pedersen TL. ggraph: An Implementation of Grammar of Graphics for Graphs and Networks. 2024.

32. Yadav S, Koenen M, Bale NJ *et al.* Organic matter degradation in the deep, sulfidic waters of the Black Sea: insights into the ecophysiology of novel anaerobic bacteria. *Microbiome* 2024;**12**:98.

33. Huber R, Hannig M. Thermotogales. In: Dworkin M, Falkow S, Rosenberg E, et al. (eds.). *The Prokaryotes: Volume 7: Proteobacteria: Delta, Epsilon Subclass*. New York, NY: Springer, 2006, 899–922.

34. Johnson MR, Conners SB, Montero CI *et al.* The Thermotoga maritima Phenotype Is Impacted by Syntrophic Interaction with Methanococcus jannaschii in Hyperthermophilic Coculture. *Appl Environ Microbiol* 2006;**72**:811–8.

35. St-Pierre B, Wright A-DG. Metagenomic analysis of methanogen populations in three full-scale mesophilic anaerobic manure digesters operated on dairy farms in Vermont, USA. *Bioresour Technol* 2013;**138**:277–84.

36. Ni J, Hatori S, Wang Y *et al.* Uncovering Viable Microbiome in Anaerobic Sludge Digesters by Propidium Monoazide (PMA)-PCR. *Microb Ecol* 2020;**79**:925–32.

37. Sun L, Pope PB, Eijsink VGH *et al.* Characterization of microbial community structure during continuous anaerobic digestion of straw and cow manure. *Microb Biotechnol* 2015;**8**:815–27.

38. Yokoyama H, Wagner ID, Wiegel J. Caldicoprobacter oshimai gen. nov., sp. nov., an anaerobic, xylanolytic, extremely thermophilic bacterium isolated from sheep faeces, and proposal of Caldicoprobacteraceae fam. nov. *Int J Syst Evol Microbiol* 2010;**60**:67–71.

39. Shaw AJ, Hogsett DA, Lynd LR. Identification of the [FeFe]-Hydrogenase Responsible for Hydrogen Generation in Thermoanaerobacterium saccharolyticum and Demonstration of Increased Ethanol Yield via Hydrogenase Knockout. *J Bacteriol* 2009;**191**:6457–64.

40. Zavarzina DG, Tourova TP, Kuznetsov BB *et al.* Thermovenabulum ferriorganovorum gen. nov., sp. nov., a novel thermophilic, anaerobic, endospore-forming bacterium. *Int J Syst Evol Microbiol* 2002;**52**:1737–43.

41. Dong N, Bu F, Zhou Q *et al.* Performance and microbial community of hydrogenotrophic methanogenesis under thermophilic and extreme-thermophilic conditions. *Bioresour Technol* 2018;**266**:454–62.

42. Kläring K, Just S, Lagkouvardos I *et al.* Murimonas intestini gen. nov., sp. nov., an acetate-producing bacterium of the family Lachnospiraceae isolated from the mouse gut. *Int J Syst Evol Microbiol* 2015;**65**:870–8.

43. McInerney MJ, Bryant MP, Hespell RB *et al.* Syntrophomonas wolfei gen. nov. sp. nov., an Anaerobic, Syntrophic, Fatty Acid-Oxidizing Bacterium. *Appl Environ Microbiol* 1981;**41**:1029–39.

44. Maus I, Cibis KG, Bremges A *et al.* Genomic characterization of Defluviitoga tunisiensis L3, a key hydrolytic bacterium in a thermophilic biogas plant and its abundance as determined by metagenome fragment recruitment. *J Biotechnol* 2016;**232**:50–60.

45. Savant DV, Ranade DR. Application of Methanobrevibacter acididurans in anaerobic digestion. *Water Sci Technol* 2004;**50**:109–14.

46. Li K, Gong H, Liu Y *et al.* Hydrogenotrophic methanogenic granular sludge formation for highly efficient transforming hydrogen to CH4. *J Environ Manage* 2022;**303**:113999.

47. Yang B, Wang C, Zhao X *et al.* Effects of environmental factors on low temperature anaerobic digestion of pig manure. *Environ Res Commun* 2022;**4**:125006.

48. Lang K, Schuldes J, Klingl A *et al.* New Mode of Energy Metabolism in the Seventh Order of Methanogens as Revealed by Comparative Genome Analysis of “Candidatus Methanoplasma termitum.” *Appl Environ Microbiol* 2015;**81**:1338–52.